



Using FEM-AI Technique to Predict the Behavior of Strip Footing Rested on Undrained Clay Layer Improved with Replacement and Geo-Grid

Ahmed M. Ebid ^{1*}, Kennedy C. Onyelowe ^{2,3}, Mohamed Salah ⁴, Edward I. Adah ⁵

¹ Faculty of Engineering and Technology, Future University in Egypt, New Cairo 11865, Egypt.

² Department of Civil Engineering, Michael Okpara University of Agriculture, Umudike, Nigeria.

³ Department of Civil Engineering, University of Peloponnese, GR-26334, Patras, Greece.

⁴ Faculty of Engineering, Ain Shams University, Cairo, Egypt.

⁵ Department of Civil and Environmental Engineering, University of Calabar, Calabar, Nigeria.

Received 02 December 2022; Revised 17 March 2023; Accepted 04 April 2023; Published 01 May 2023

Abstract

The objective of this research is to predict how strip footings behave when rested on an undrained clay layer enhanced using a top replacement layer with and without a geo-grid. The study was conducted in several stages, including collecting load-settlement curves from "Finite Element Method" (FEM) models with different clay strengths, replacement thicknesses, and axial stiffnesses of the geo-grid. These curves were then idealized using a hyperbolic model, and the idealized hyperbolic parameters were predicted using three different AI techniques. According to the numerical results, the ultimate bearing pressure of pure clay models was found to be five times the undrained strength of the clay. These findings align with most established empirical bearing capacity formulas for undrained clays. The results also suggest that the initial modulus of the subgrade reaction is solely influenced by replacement thickness. Additionally, the enhancement in subgrade reaction due to the replacement layer decreases with increasing clay strength. However, the percentage of improvement decreased with higher clay strength. Moreover, the impact of the geo-grid was significant for settlement beyond 50mm, and it was more impactful in soft clay than in stiff clay. Finally, the research proposed predictive models employing the "Genetic Programming" (GP), "Artificial Neural Networks" (ANN), and "Evolutionary Polynomial Regression" (EPR) techniques, and these models exhibited an accuracy of about 88%.

Keywords: Strip Footing; Undrained Clay; Geo-Grid; FEM; AI; Subgrade Reaction.

1. Introduction

The determination of soil subgrade reaction is crucial in the design of continuous shallow foundations such as strip footings and rafts. This factor dictates the amount of weight that causes the unit settlement and consequently affects the type and size of the foundations. The issue of the behavior of strip footings (load-settlement curve) is a fundamental and classic problem in geotechnical engineering. It is often used to determine the bearing capacity of clay soils. The allowable bearing capacity of clays, silty clays, and plastic silts may be restricted by either the requirement for an adequate safety factor against shear and failure or by considerations related to settlement [1].

Geosynthetics have a wide range of applications, including separation, protection, drainage, filtration, reinforcement, and sealing. These materials are designed to serve specific functions. For example, geo-membranes are used for containment, geogrids for reinforcement, and geotextiles for a variety of purposes, such as filtration, drainage,

* Corresponding author: ahmed.abdelkhaleq@fue.edu.eg

 <http://dx.doi.org/10.28991/CEJ-2023-09-05-014>



© 2023 by the authors. Licensee C.E.J, Tehran, Iran. This article is an open access article distributed under the terms and conditions of the Creative Commons Attribution (CC-BY) license (<http://creativecommons.org/licenses/by/4.0/>).

separation, protection, and reinforcement [2–4]. Geogrids are particularly effective in providing reinforcement and stability to structures such as retaining walls, pavements, foundations, slopes, and embankments due to their high tensile strength. They are created by the interlocking of tensile elements with openings large enough to allow for interlocking with nearby fill materials [5-8].

The ultimate bearing capacity is the extreme point in the load-settlement curve; this has been extensively studied by many researchers using different methods. For example, Das et al. [9] experimentally compared the enhancement in bearing capacity of strip footing rested on sand and clay layers when they are reinforced with geo-grid; Arvin et al. [10] utilized shakedown theory to determine the static and dynamic bearing capacity of strip footings under varying repeated loads; and Gnananandarao et al. [11] numerically studied the bearing capacity of multi-edge skirted footings resting on sand. Finally, Ebid et al. estimated the bearing capacity of strip footing nearing or within slopes [12] and resting on multi-layered soil [13] using different AI techniques. Generally, all previous literature agreed that the ultimate bearing capacity of strip footing rested on pure undrained clay and subjected to a centric vertical load is about five times the undrained shear strength of the clay [14].

Unlike the ultimate bearing capacity, the subgrade reaction is not limited to the extreme point of the load-settlement curve; it presents the slope of the curve, and hence, its value varies with the applied load. Many researchers suggested different approaches to estimating the value of the subgrade reaction. Christopher et al. [15] measured the subgrade reaction of roadway bases strengthened with geosynthetics. Biswas et al. [16] numerically estimated the value of the subgrade reaction for a shallow foundation rested on a clay layer reinforced using geo-grid of different lengths. Aboelela et al. [17] developed a mathematical formula to estimate the subgrade reaction at the bed of deep excavation in sand using the GP technique. Onyelowe et al. [18] presented three AI-based predictive models to estimate the values of some parameters of HSDA-treated black cotton clay, including the subgrade reaction. Kazi et al. [19] experimentally observed the behavior of shallow footings resting on a sand layer provided with geotextile. Tafreshi et al. [20] used both lab tests and FEM models to investigate the behavior of shallow footing resting on multi-layered rubber-reinforced soil. Finally, Mahdi et al. [21] used the same techniques to estimate the lateral subgrade reaction of multi-layered soil.

The previous research used either lab tests or FEM or both to predict the full load-settlement curve of a shallow footing rested on soil; however, there are many different FEM and AI models to predict the ultimate bearing capacity. That indicated the need for models that could be manually used (closed-form equations) to predict the full behavior (i.e., load-settlement curve) of shallow footing resting on the soil. Hence, this study aims to introduce three artificial intelligence (AI) models that can predict the full behavior of a strip footing founded on a clay layer enhanced using a top replacement layer with or without a geo-grid. The considered AI techniques are ANN, GP, and EPR.

2. Research Methodology

The research plan is comprised of three phases. In Phase-1, 30 FEM models are developed for strip footing resting on a clay layer that is improved with a replacement layer (with or without geo-grid). These models are used to determine the load corresponding to settlements of 50, 100, 150, 200, and 250 mm, as well as the ultimate load and settlement. In Phase-2, the (a & b) factors for the best-fitting hyperbolic curve are calculated for the output of each FEM model. A database is then formed, which contains the configurations of each FEM model and the corresponding a & b values. Finally, in Phase-3, different AI techniques are applied to the generated database to predict the a & b values using the model configurations. The following section provides a detailed description of each phase of the research. The methodology considered in this research is graphically presented in Figure 1.

2.1. Phase-1: FEM Models

In the parametric study, a total of thirty 2D plain strain PLAXIS [22] models were developed for a strip footing with a width of 1.0 m resting on a half space clay layer with a total thickness of 10.0 m. To investigate the effect of replacement, the surface layer at depths of 0.5, 1.0, and 1.5 m (depth/width = 0.0, 0.5, 1.0, 1.5) was replaced with dense sand with or without a geo-grid, as illustrated in Fig 2. The problem was modelled with symmetry, and only half of the model was used. The finite element mesh used a 15-node element. To ensure that the boundary conditions did not restrict soil movement due to the footing load, the size of the finite element model was chosen to be large enough (10 ×10 m) and in agreement with previous research approaches [23, 24]. The soil layers were modelled using Mohr-Coulomb's constitutive law with parameters listed in Table 1 and Figure 2.

Table 1. Element parameters used in FEM models

Element Type	Description	C (kN/m ²)	φ (°)	γ' (kN/m ³)	E (kN/m ²)	ν
Rep	Replacement	0.0	38.0	10.0	50000	0.30
C25	Undrained Soft Clay	25.0	0.0	10.0	2000	0.45
C50	Undrained Medium Clay	50.0	0	10.0	4500	0.40
C100	Undrained Stiff Clay	100.0	0	10.0	10000	0.35
Geo20	Geo-grid (T 2% = 20 kN/m)				Axial stiffness = 1.0 MN/m	
Geo40	Geo-grid (T 2% = 40 kN/m)				Axial stiffness = 2.0 MN/m	

where C , ϕ , γ' , E , ν are the cohesion, friction angle, effective unit weight, elastic modulus and Poisson's ratio of the soil respectively.

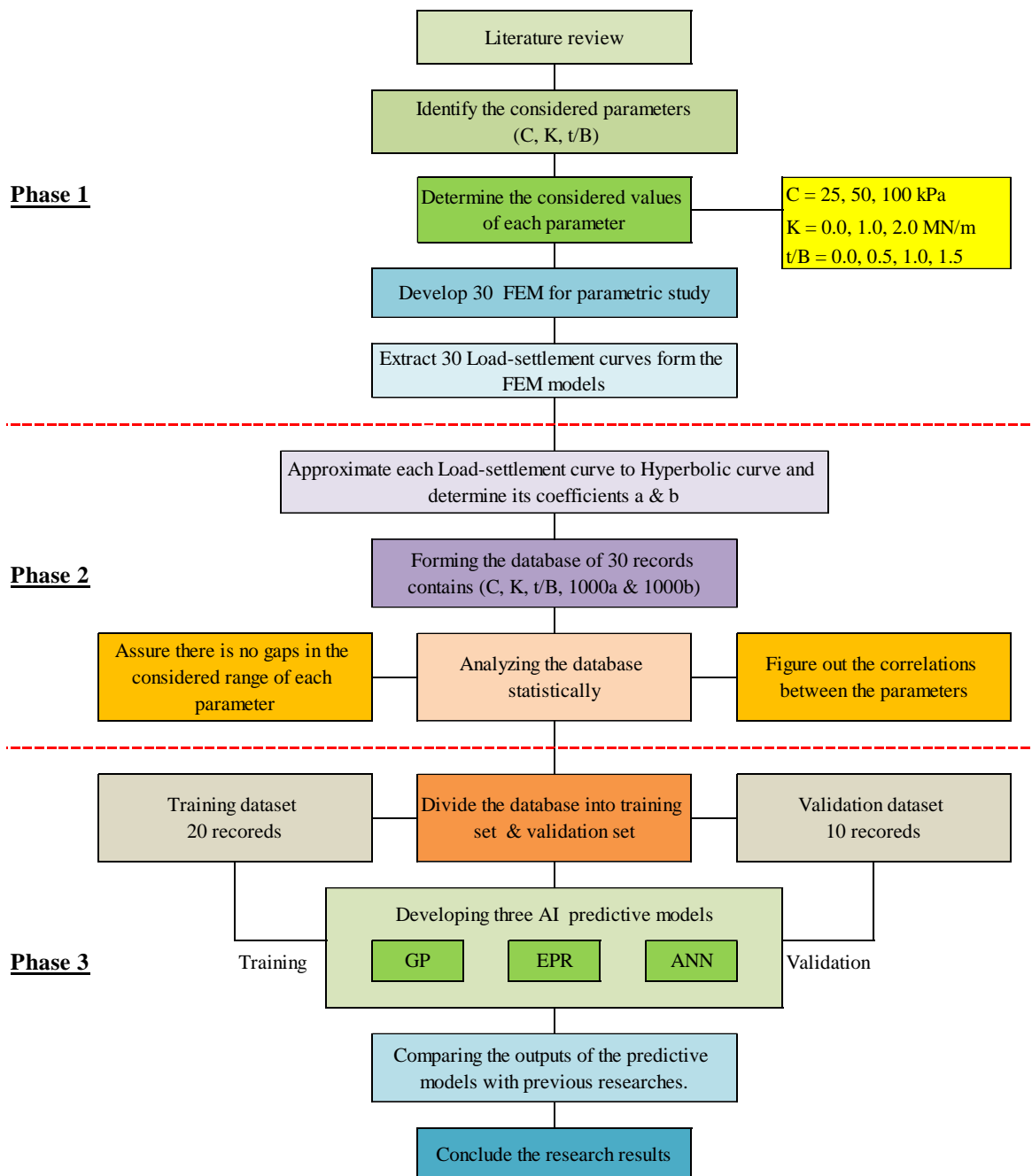


Figure 1. The considered methodology in this research

To evaluate the impact of clay strength, replacement depth/footing width, and stiffness of geo-grid on load-settlement curves, thirty FEM models were developed with different combinations of these three parameters. The considered values of each parameter were:

- Undrained clay strength (soft $C=25$ kPa, medium $C=50$ kPa & stiff $C=100$ kPa);
- Replacement depth / footing width (t/B) (0.0, 0.5, 1.0 ,1.5);
- Axial stiffness of geo-grid (K) (0.0, 1.0, 2.0 MN/m).

For each FEM model, the corresponding loads to settlement values of 50, 100, 150, 200 and 250 mm were recorded in addition to the ultimate load and its corresponding settlement.

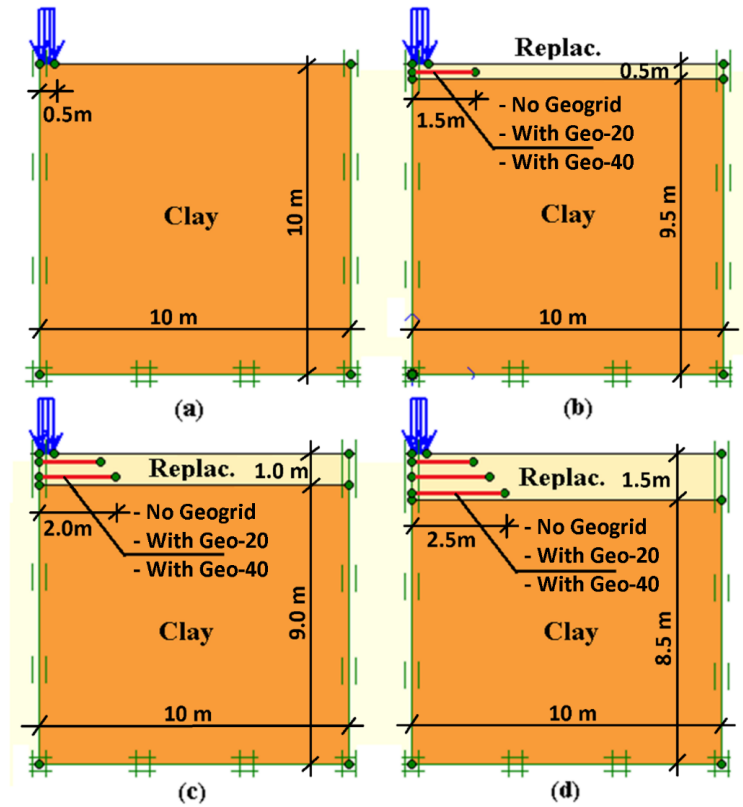


Figure 2. The developed FEM models (a) Pure Clay (b), (c) & (d) improved clay with replacement layer (depth/width = 0.5, 1.0, 1.5) respectively with and without geo-grid

Figure 3 shows an example of the FEM outputs. It shows a comparison between the ultimate deviatoric stress (q) for pure soft clay: soft clay with a 0.5m thick replacement layer included one layer of Geo20, soft clay with a 1.0m thick replacement layer included two layers of Geo20, and soft clay with a 1.5m thick replacement layer included three layers of Geo20. The comparison illustrates the increase in ultimate deviatoric stress (i.e., shear strength) with increasing enhancing materials (replacement and geogrid).

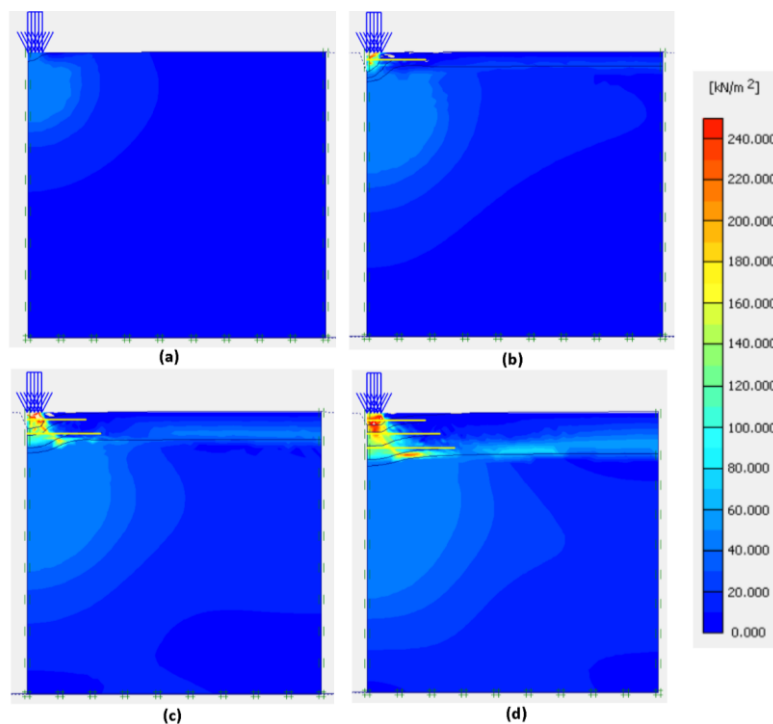


Figure 3. Example for the FEM output, comparison between the ultimate deviatoric stress (q) for a) Pure soft clay, b) soft clay+0.5 Repl.+Geo20, c) Soft clay+1.0 Repl.+Geo20, d) soft clay+1.5 Repl.+Geo20

The full outcomes of phase-1 are the thirty (load-settlement) curves from the developed FEM models, which are summarized in Figure 4.

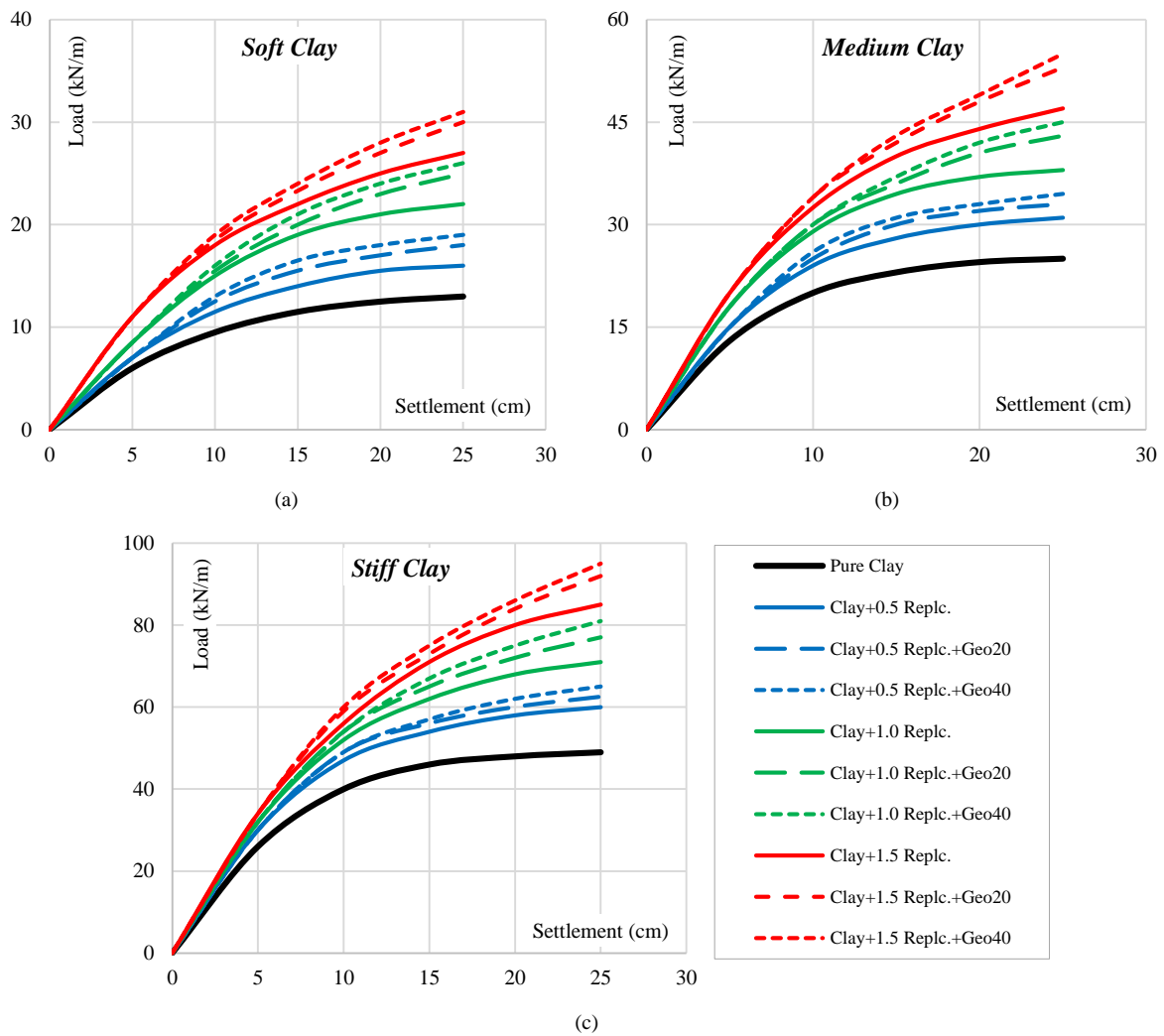


Figure 4. Load – settlement curves from developed FEM models, a) soft clay, b) medium clay & c) stiff clay

2.2. Phase-2: Calculate (a & b) Factors & Forming the Database

The hyperbolic formula is a commonly used method to describe the relationship between load and settlement in geotechnical models like pile load tests and plate load tests. Therefore, this study also uses the hyperbolic formula to describe the results of the FEM models. By using only two factors (a and b), the best-fitting hyperbolic curve for a set of results can be determined, as illustrated in Figure 5.

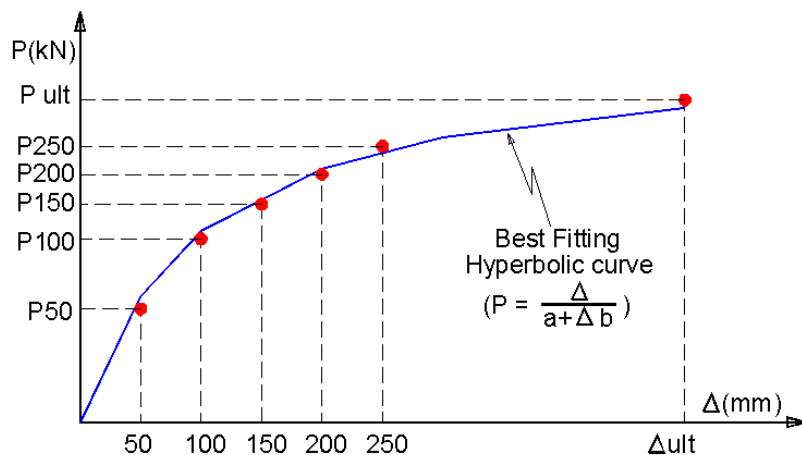


Figure 5. Best fitting hyperbolic curve

The optimum values for (a & b) parameters are the values that minimize the "Sum of Squared Error" (SSR) between the FEM results and the corresponding points on the hyperbolic curve. This optimization was done using a built-in function in the widely used MS-EXCEL software. A dataset consisting of 30 records was created for use by the AI techniques, with each record containing the following data:

- Cohesion of clay layer (C) kPa,
- Replacement depth/footing width (t/B),
- Axial stiffness of geo-grid (K) MN/m,
- $1000 \times$ hyperbolic factor (a),
- $1000 \times$ hyperbolic factor (b).

The dataset created was split into two sets: training and validation sets, consisting of 20 and 10 records, respectively. Tables 2 and 3 provide an overview of the statistical characteristics of the dataset, as well as the correlation matrix, while Figure 6 illustrates the statistical distribution, presented as histograms, of the input and output parameters. The full databases are available in the appendix I.

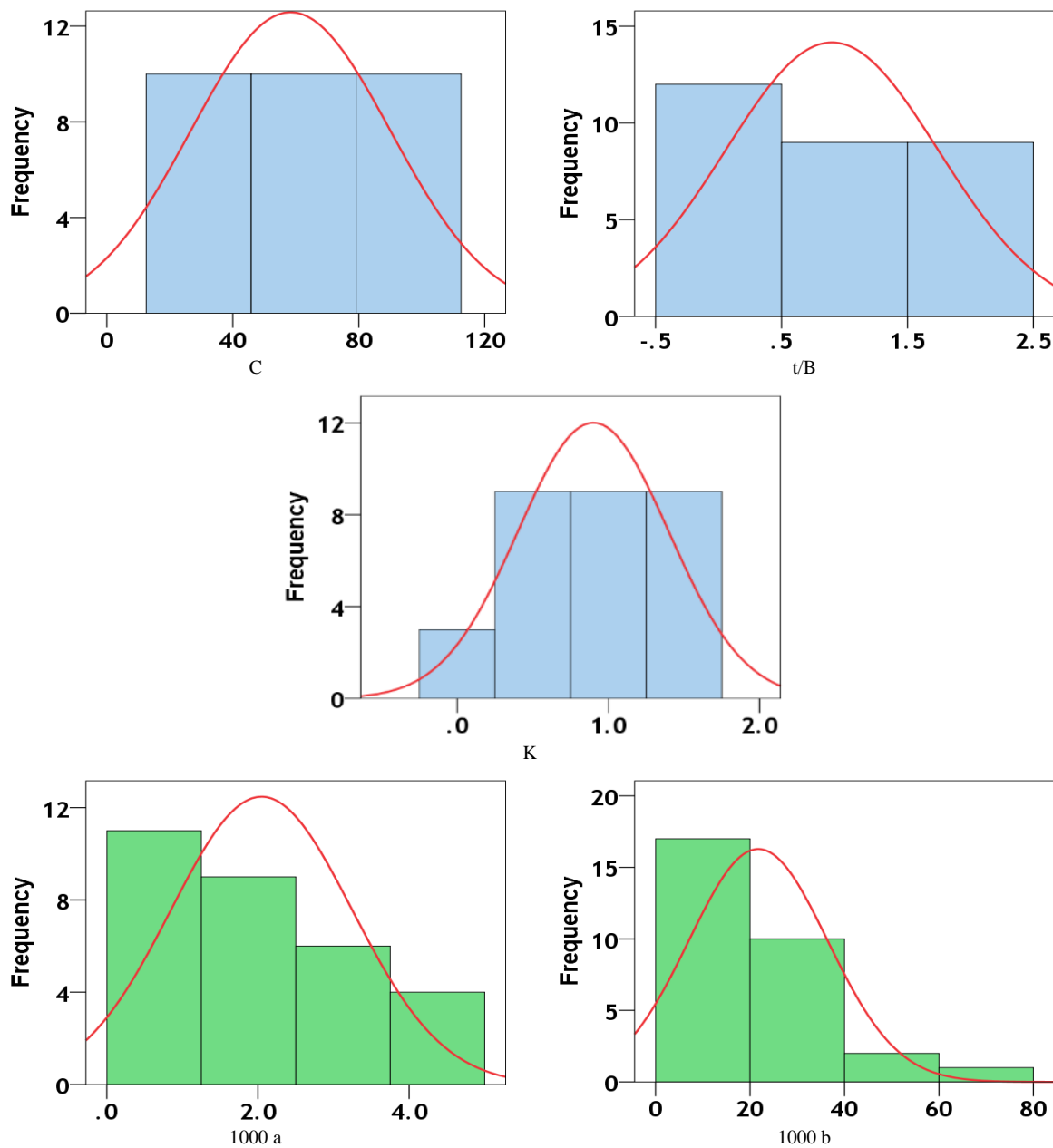


Figure 6. Distribution histograms for inputs (in blue) and outputs (in green)

Table 2. Statistical analysis of generated database

	C (kPa)	t/B -	K (kN/m)	1000a (m/kPa)	1000b (1/kN)
Training set					
Min.	25.00	0.00	0.00	1.09	10.45
Max.	100.00	2.00	1.50	4.15	71.46
Avg.	63.75	0.65	0.85	2.64	27.07
SD	31.10	0.65	0.53	1.01	14.86
VAR	0.49	1.01	0.62	0.38	0.55
Validation set					
Min.	25.00	0.00	0.50	0.51	7.28
Max.	100.00	2.00	1.50	1.09	19.41
Avg.	47.50	1.40	1.00	0.86	11.02
SD	28.39	0.92	0.39	0.16	3.56
VAR	0.60	0.65	0.39	0.18	0.32

Table 3. Correlation matrix

	C	K	t/B	1000a	1000b
C	1.000				
K	0.000	1.000			
t/B	0.000	0.221	1.000		
1000a	-0.882	0.117	0.107	1.000	
1000b	-0.635	-0.292	-0.595	0.524	1.000

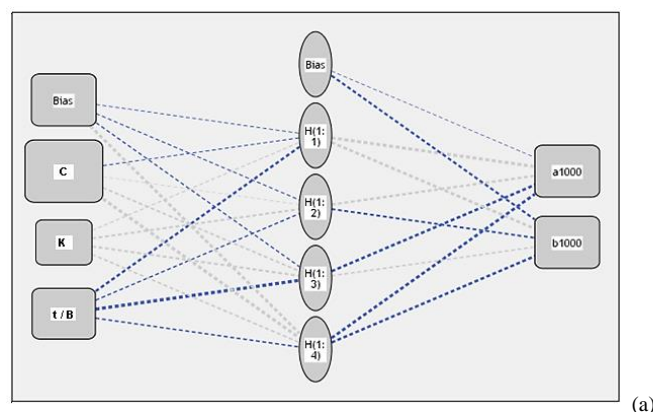
2.3. Phase-3: Predicting (a and b) Values using AI Techniques

Three different AI techniques were utilized to predict the hyperbolic factors (a and b) of the load-settlement curve of strip footing using the generated database. The techniques used were "Evolutionary Polynomial Regression" (EPR), "Artificial Neural Network" (ANN), and "Genetic Programming" (GP). These models were designed to forecast the values of (a and b) based on three inputs: undrained clay cohesion (C), replacement depth/footing width (t/B), and axial stiffness of the geo-grid (K). To evaluate the accuracy of each model, the "Sum of Squared Errors" (SSE) was utilized.

2.3.1. (ANN) Model

"Artificial Neural Network" ANN is a type of machine learning algorithm inspired by the structure and function of the human brain. ANN is widely used in various fields, including image and speech recognition, natural language processing, and prediction modeling. It consists of interconnected processing nodes that can learn to recognize patterns and relationships in data through the use of training algorithms. ANN can be used for both supervised and unsupervised learning tasks and has the ability to generalize and make predictions on unseen data [25].

Using "Back Propagation" (BP) technique, a single hidden layer (ANN) with a non-linear activation function (Hyper-Tan) was trained to predict the values of (a and b) factors. The structure of the developed ANN and the connection weights are shown in Figure 7 and Table 4. The average errors were 8.8% and 12.9%, and the R² values were 0.978 and 0.961. The relationship between the calculated and predicted values is illustrated in Figures 8-c and 9-c.



(a)

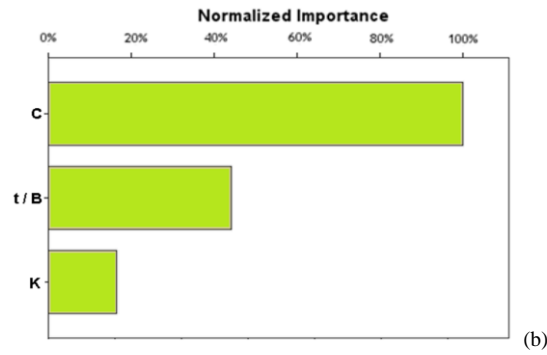


Figure 7. The developed ANN (a) layout, (b) Normalized importance of inputs

Table 4. Weights matrix for the developed ANN model

		Hidden Layer 1				Output Layer	
		H(1:1)	H(1:2)	H(1:3)	H(1:4)	a1000	b1000
Input Layer	(Bias)	-0.09	-0.16	-0.25	1.05		
	C	-0.14	0.04	0.38	1.92		
	K	0.19	0.59	0.59	0.36		
	t/B	-0.64	-0.26	-2.21	-0.27		
Hidden Layer 1	(Bias)					0.00	-0.60
	H(1:1)					1.16	0.96
	H(1:2)					0.61	-0.56
	H(1:3)					-0.73	0.32
	H(1:4)					-0.97	-0.71

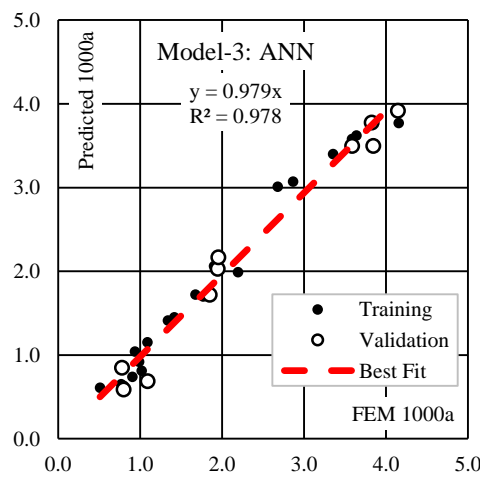
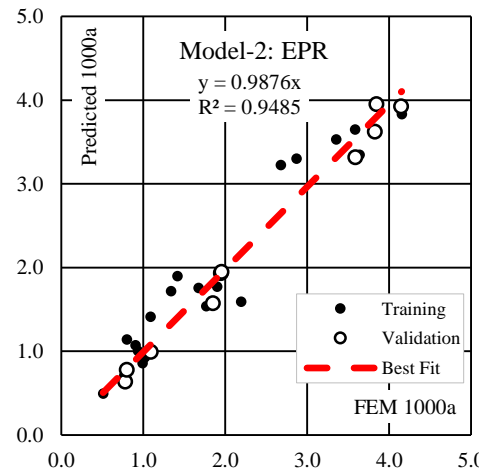
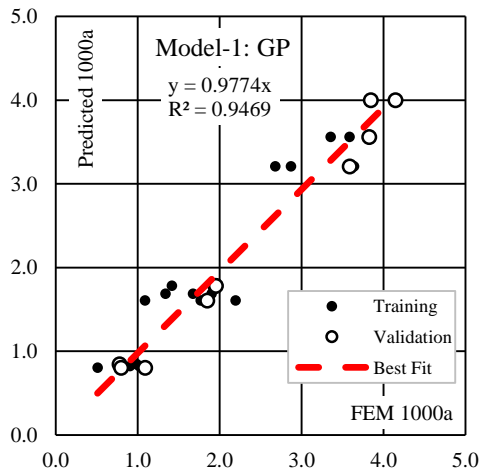


Figure 8. Predicted Vs. calculated (1000a) values

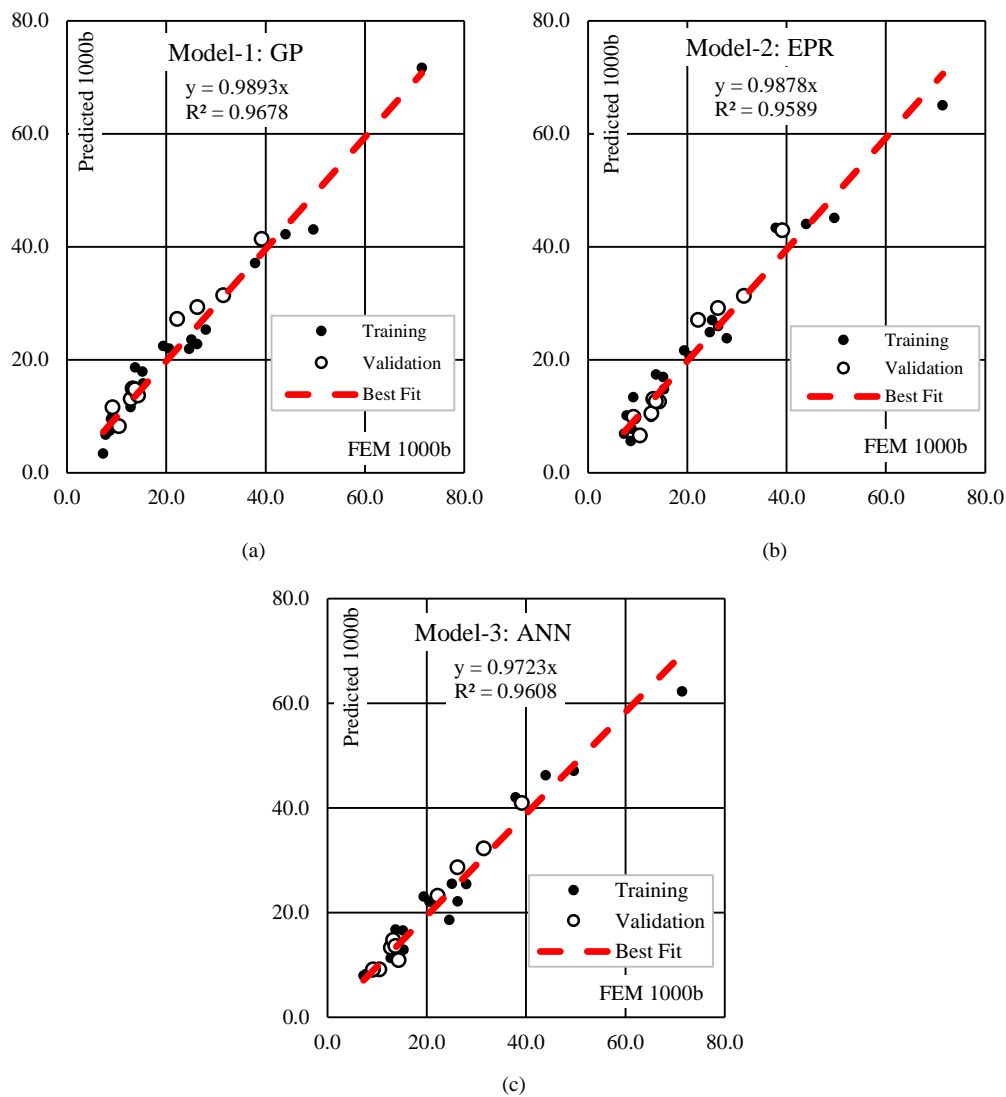


Figure 9. Predicted Vs. calculated (1000b) values

2.3.2. (GP) Model

“Genetic Programming” (GP) is a subfield of AI that is based on the principles of natural selection and genetic evolution. It is a machine learning technique that uses a population-based approach to find a solution to a problem by creating and evolving computer programs. In GP, solutions are represented as formulas that are evolved over multiple generations through the application of genetic operators such as selection, mutation, and crossover. The best solutions are selected through a fitness function that evaluates their performance on a given task, and these solutions are used to create the next generation of programs [26].

A GP model with two levels of complexity, consisting of 31 genes per chromosome, was developed to predict the (a and b) values of the generated database records. This model was developed using a population size of 100,000 chromosomes, a survivor size of 25,000 chromosomes, and 250 generations. Equations 1 and 2 present the generated formulas for (a and b), while Figures 8-a and 9-a show their fitness. The average error and R² values for this model were 13.3%, 0.947, and 11.7%, 0.968, respectively.

$$1000 a = \frac{80}{C-2.5 K} \tag{1}$$

$$1000 b = \frac{8.45 C+1100}{C(t/B+0.9)-4.3} - [(1.47K - 0.8)(1.7t/B - 0.28)] \tag{2}$$

2.3.3. (MPR) Model

“Evolutionary Polynomial Regression” (EPR) is a machine learning technique used for regression analysis to model complex relationships between variables. It involves evolving polynomial equations using a genetic algorithm, where the polynomial terms and their coefficients are determined simultaneously. EPR can handle a large number of variables and interactions among them and has been applied in various fields. The main advantage of EPR is its ability to find the simplest equation that best fits the data, providing insights into the underlying relationships between variables [27].

A second-order EPR model was constructed with three inputs, resulting in a total of 10 possible combinations ($6+3+1=10$), including:

$$\sum_{i=1}^{i=3} \sum_{j=1}^{j=3} X_i \cdot X_j + \sum_{i=1}^{i=3} X_i + C \quad (3)$$

The "Genetic Algorithm" (GA) technique was employed to select the seven most important terms out of the ten possible terms of the traditional quadratic polynomial. The resulting models for predicting the values of (a and b) are presented in Equations 3 and 4, and their fitness values are illustrated in Figures 8-b and 9-b. The determination factor (R^2) and average error values are 0.949, 12.8%, and 0.959, 13.3%, respectively.

$$1000a = 6.14 - C \left[\frac{1}{7.5} + \frac{K}{200} - \frac{t}{155B} - \frac{C}{1313} \right] + \frac{K}{2.32} - \left(\frac{t}{2.66B} \right)^2 \quad (4)$$

$$1000b = 94.0 + \frac{t}{B} \left[\frac{C}{13.33} + 12.5 \frac{t}{B} - 2.14 Kg - 53.5 \right] + C \left[\frac{C}{172} - 1.3 \right] \quad (5)$$

3. Results and Discussion

3.1. Phase-1

During Phase-1, the results presented in Figure 4 demonstrated the load-settlement curves of each FEM model developed. Analyzing these curves highlighted the following observations:

- The ultimate bearing pressure of models consisting of pure clay is found to be five times the undrained cohesion strength of the clay. This result aligns with most of the established empirical bearing capacity formulas for cohesive soil (C-soil).
- The initial slope of the curves is constant for a given replacement thickness, irrespective of the axial stiffness of the geo-grid. This implies that the initial modulus of subgrade reaction up to a settlement of 50mm is solely dependent on the replacement thickness.
- The modulus of subgrade reaction increases as the replacement thickness increases, regardless of the clay strength. However, the rate of improvement decreases with increasing clay strength. For instance, with a replacement thickness to footing width (t/B) ratio of 1.5, the improvement percentages were 200%, 150%, and 133% for soft, medium, and stiff clay, respectively.
- Beyond the 50 mm settlement, a noticeable effect of the geo-grid can be observed. The extent of improvement in the footing behavior increases with an increase in the axial stiffness of the geo-grid, regardless of the replacement thickness or clay strength.
- The contribution of geo-grid is more effective in soft clay compared to stiff clay. For instance, when settling at 250mm, the bearing stress was enhanced by 200%, 133%, and 125% for soft, medium, and stiff clay, respectively, when using Geo-40.
- Overall, the addition of replacement material, with or without geo-grid, improves the performance of clayey soil by increasing both the ultimate bearing capacity and ultimate settlement. In comparison, pure clay failed at a settlement of 250mm, while the ultimate settlements of clay reinforced with replacement material, with and without geo-grid, were approximately 600mm and 750mm, respectively. As a result, the design of such footings will be governed by settlement criteria.

3.2. Phase-2

During Phase-2, a mathematical model was utilized to describe the load-settlement curve with minimal variables. The authors chose the well-known hyperbolic model since it only necessitates two parameters, namely (a and b), to characterize the curve. Furthermore, this model can replicate the decrease in soil stiffness with loading until failure. The values of both (a and b) were determined for each load-settlement curve using the criteria of least squares error.

The hyperbolic model comprises two parameters, each with a specific meaning. Parameter (a) represents the inverse of the initial slope of the curve, which is the inverse of the initial subgrade reaction. Parameter (b) represents the upper value of the curve, where the ultimate bearing stress is equal to $1/(1.2 b)$.

3.3. Phase-3

During Phase-3, a dataset of 30 records, each comprising values of C, t/B , K, 1000a, and 1000b, was generated, and three AI techniques, namely GP, EPR, and ANN, were employed. Due to the small values of (a and b) when compared to other parameters, 1000a and 1000b were used to ensure calculation stability. The output of each technique was evaluated as follows:

- All of the developed AI models demonstrated a comparable level of accuracy, with an average error ranging from 12 to 13%. However, the ANN model for 1000a exhibited a lower average error of 8.8%.
- The normalized importance chart in Figure 7-b showed that the clay strength has the most significant impact on the footing behavior, followed by the replacement thickness and, finally, the axial stiffness of the geo-grid. This finding is consistent with the previous analysis in Phase-1.
- The equation generated by the GP model (Equation 1) revealed that the initial subgrade reaction is primarily influenced by the clay strength, which is consistent with the findings of Phase-1.
- Table 5 summarizes the accuracy levels of the developed models, while their fitness is graphically presented in Figures 8 and 9.

Table 5. Accuracies of developed models

Item	Technique	Output	SSE	Avg. Error	R ²
1000a	GP	Equation 1	2.21	13.3	0.947
	EPR	Equation 3	2.07	12.8	0.949
	ANN	Figure 6	0.98	8.8	0.978
1000b	GP	Equation 2	194.0	11.7	0.968
	EPR	Equation 4	250.0	13.3	0.959
	ANN	Figure 6	237.0	12.9	0.961

4. Conclusions

The main objective of this study is to predict the behavior of strip footings resting on clay soil that has been improved using replacement with different thicknesses, with and without the use of geo-grid. The methodology comprises three phases. The first phase involves collecting load-settlement curves from FEM models with varying clay strengths, replacement thicknesses, and axial stiffness of the geo-grid. The second phase entails the use of hyperbolic models to idealize the collected curves. Finally, in the third phase, three AI techniques (GP, ANN, and EPR) are employed to predict the idealized hyperbolic parameters. The key findings of this research are summarized as follows:

- The initial subgrade reaction value (for settlement up to 50 mm) mainly increases as the thickness of the replacement layer increases. This improvement is more pronounced for soft clay and decreases for stiffer clays.
- The contribution of the geo-grid to enhancing the subgrade reaction becomes significant beyond a settlement of 50mm, and the effect is more pronounced with an axially stiffer geo-grid.
- The use of geo-grid results in delaying the shear failure, leading to a significant increase in ultimate settlement values. Therefore, in such cases, the allowable bearing stress is governed by the settlement criteria.
- Using the FEM-AI technique, three predictive models were developed that can accurately forecast the behavior (load-settlement curve) of a strip footing resting on an undrained clay layer that has been improved with a surface replacement layer with or without geo-grid, with an accuracy of approximately 88%.
- The predicted load-settlement curve could be used to identify the subgrade reaction value for a certain load as well as the ultimate bearing stress and the corresponding ultimate settlement.
- The validity of all the generated models is limited by the range of input parameter values considered. For any values beyond this range, the accuracy of predictions should be verified.

5. Declarations

5.1. Author Contributions

Conceptualization, A.M.E.; methodology, A.M.E.; formal analysis, M.S.; investigation, M.S.; data curation, E.I.A.; writing—review and editing, A.M.E., K.C.O., M.S., and E.I.A.; supervision, K.C.O. All authors have read and agreed to the published version of the manuscript.

5.2. Data Availability Statement

The data presented in this study are available on request from the corresponding author.

5.3. Funding

The authors received no financial support for the research, authorship, and/or publication of this article.

5.4. Conflicts of Interest

The authors declare no conflict of interest.

6. References

- [1] Craig, R. F. (1994). *Soil Mechanics*. Chapman & Hall, London, United Kingdom.
- [2] Kelsey, C. (2014). A brief history of geotextile. *Land and Water: Geotextiles*, 1-6. Available online: https://www.geosynthetica.com/wp-content/uploads/Kelsey_GeotextileHistory_April2014.pdf (accessed on April 2023).
- [3] Henry, K. S., & Stormont, J. C. (2002). Geocomposite capillary barrier drain for limiting moisture changes in pavement subgrades and base courses. No. NCHRP-IDEA Project 68, Transportation Research Board, Washington, United States.
- [4] McCartney, J. S., Kuhn, J. A., & Zornberg, J. G. (2005). Geosynthetic drainage layers in contact with unsaturated soils. *Proceedings of the 16th International Conference on Soil Mechanics and Geotechnical Engineering*. doi:10.3233/978-1-61499-656-9-2301.
- [5] Zornberg, J. G. (1994). Performance of geotextile-reinforced soil structures. Ph.D. Thesis, University of California, Berkeley, United States.
- [6] Zornberg, J. G., & Thompson, N. (2012). Application guide and specifications for geotextiles in roadway applications. No. FHWA/TX-10/0-5812-1, Center for Transportation Research, University of Texas, Austin, United States.
- [7] Ziegler, M. (2017). Application of Geogrid Reinforced Constructions: History, Recent and Future Developments. *Procedia Engineering*, 172, 42–51. doi:10.1016/j.proeng.2017.02.015.
- [8] Balaji, D. S., Vinodhkumar, S., & Ridhuvarsine, R. G. (2019). Applications and Performance of Geogrids in Structures. *International Journal of Recent Technology and Engineering (IJRTE)*, 8(4), 5495–5500. doi:10.35940/ijrte.d8831.118419.
- [9] Das, B. M., Shin, E. C., & Omar, M. T. (1994). The bearing capacity of surface strip foundations on geogrid-reinforced sand and clay - a comparative study. *Geotechnical and Geological Engineering*, 12(1), 1–14. doi:10.1007/BF00425933.
- [10] Arvin, M. R., Askari, F., & Farzaneh, O. (2012). Static and dynamic bearing capacity of strip footings, under variable repeated loading. *Turkish Journal of Engineering and Environmental Sciences*, 36(1), 19–31. doi:10.3906/muh-1011-22.
- [11] Gnananandarao, T., Khatri, V. N., & Dutta, R. K. (2020). Bearing capacity and settlement prediction of multi-edge skirted footings resting on sand. *Ingenieria e Investigacion*, 40(3), 9–21. doi:10.15446/ing.investig.v40n3.83170.
- [12] Ebid, A. M., Onyelowe, K. C., & Arinze, E. E. (2021). Estimating the Ultimate Bearing Capacity for Strip Footing Near and within Slopes Using AI (GP, ANN, and EPR) Techniques. *Journal of Engineering*, 2021, 1–11. doi:10.1155/2021/3267018.
- [13] Ebid, A. M., Onyelowe, K. C., & Salah, M. (2022). Estimation of Bearing Capacity of Strip Footing Rested on Bilayered Soil Profile Using FEM-AI-Coupled Techniques. *Advances in Civil Engineering*, 2022, 1–11. doi:10.1155/2022/8047559.
- [14] Das, B. M., & Sivakugan, N. (2018). *Principles of foundation engineering*. Cengage learning, Boston, United States.
- [15] Christopher, B. R., Hayden, S. A., & Shao, A. (2000). Roadway base and subgrade geocomposite drainage layers. No. STP 1390, American Society for Testing and Materials (ASTM), Pennsylvania, United States.
- [16] Biswas, A., Asfaque Ansari, M., Dash, S. K., & Murali Krishna, A. (2015). Behavior of Geogrid Reinforced Foundation Systems Supported on Clay Subgrades of Different Strengths. *International Journal of Geosynthetics and Ground Engineering*, 1(3). doi:10.1007/s40891-015-0023-5.
- [17] Aboelela, A. E., Ebid, A. M., & Fayed, A. L. (2022). Estimating the subgrade reaction at deep braced excavation bed in dry granular soil using genetic programming (GP). *Results in Engineering*, 13. doi:10.1016/j.rineng.2021.100328.
- [18] Onyelowe, K. C., Aneke, F. I., Onyia, M. E., Ebid, A. M., & Usungedo, T. (2022). AI (ANN, GP, and EPR)-based predictive models of bulk density, linear-volumetric shrinkage & desiccation cracking of HSDA-treated black cotton soil for sustainable subgrade. *Geomechanics and Geoengineering*, 1–20. doi:10.1080/17486025.2022.2090621.
- [19] Kazi, M., Shukla, S. K., & Habibi, D. (2016). Behaviour of an embedded footing on geotextile-reinforced sand. *Proceedings of the Institution of Civil Engineers: Ground Improvement*, 169(2), 120–133. doi:10.1680/grim.14.00022.
- [20] Moghaddas Tafreshi, S. N., Joz Darabi, N., Tavakoli Mehrjardi, G., & Dawson, A. (2019). Experimental and numerical investigation of footing behaviour on multi-layered rubber-reinforced soil. *European Journal of Environmental and Civil Engineering*, 23(1), 29–52. doi:10.1080/19648189.2016.1262288.
- [21] Mahdi, H. A., Ebid, A. M., Onyelowe, K. C., & Nwobia, L. I. (2022). Predicting the behaviour of laterally loaded flexible free head pile in layered soil using different AI (EPR, ANN and GP) techniques. *Multiscale and Multidisciplinary Modeling, Experiments and Design*, 5(3), 225–242. doi:10.1007/s41939-021-00114-5.

- [22] Brinkgreve, R. B. J., Kumarswamy, S., Swolfs, W. M., Waterman, D., Chesaru, A., & Bonnier, P. G. (2016). PLAXIS 2016. Pennsylvania, United States.
- [23] Potts, D. M., & Zdravković, L. (2001). Finite Element Analysis in Geotechnical Engineering: Volume two - Application. Thomas Telford, London, United Kingdom. doi:10.1680/feaigea.27831.
- [24] Bartlett, S. T. (2010). Numerical methods in geotechnical engineering. Course notes, University of Utah, Salt Lake City, United States.
- [25] Aneke, F. I., Onyelowe, K. C., Ebid, A. M., Nwobia, L. I., & Adu, J. T. (2022). Predictive models of swelling stress—a comparative study between BP- and GRG-ANN. *Arabian Journal of Geosciences*, 15(17). doi:10.1007/s12517-022-10706-1.
- [26] El-Bosraty, A. H., Ebid, A. M., & Fayed, A. L. (2020). Estimation of the undrained shear strength of east Port-Said clay using the genetic programming. *Ain Shams Engineering Journal*, 11(4), 961–969. doi:10.1016/j.asej.2020.02.007.
- [27] Giustolisi, O., & Savic, D. A. (2006). A symbolic data-driven technique based on evolutionary polynomial regression. *Journal of Hydroinformatics*, 8(3), 207–222. doi:10.2166/hydro.2006.020b.

Appendix I: Generated Database

C (kPa)	K (MN/m)	t/B (-)	1000a (-)	1000b (-)
Training set				
50	1	1.50	1.7	12.8
100	0	0.00	0.5	19.4
50	2	1.00	2.0	14.3
100	1	0.50	0.8	13.3
100	0	1.00	1.1	9.2
100	1	1.00	1.0	8.9
25	0	0.50	3.6	49.6
50	0	1.50	1.8	13.2
25	0	0.00	2.9	71.5
25	0	1.50	2.7	28.0
25	2	1.50	4.2	13.7
50	0	0.50	1.8	25.1
50	0	0.00	1.1	37.9
50	2	0.50	1.4	24.6
100	2	1.50	0.9	7.3
25	1	1.50	3.4	20.6
25	2	0.50	3.8	39.2
50	0	1.00	2.2	15.2
25	1	0.50	3.6	44.0
100	0	0.50	0.8	13.7
Validation set				
25	2	1.00	4.1	22.2
25	0	1.00	3.6	31.4
100	2	0.50	0.8	12.8
100	0	1.50	0.8	9.2
50	1	0.50	1.3	26.2
50	1	1.00	1.9	15.4
50	2	1.50	1.9	10.4
100	2	1.00	1.0	8.7
100	1	1.50	0.9	7.8
25	1	1.00	3.8	26.2